J Electr Eng Technol Vol.9, No.1: 37-44, 2014
http://dx.doi.org/10.5370/JEET.2014.9.1.037

ISSN(Print) 1975-0102
ISSN(Online) 2093-7423

Robust Diagnosis Algorithm for Identifying Broken Rotor Bar Faults in Induction Motors

Don-Ha Hwang*, Young-Woo Youn*, Jong-Ho Sun* and Yong-Hwa Kim†

Abstract – This paper proposes a new diagnosis algorithm to detect broken rotor bars (BRBs) faults in induction motors. The proposed algorithm is composed of a frequency signal dimension order (FSDO) estimator and a fault decision module. The FSDO estimator finds a number of fault-related frequencies in the stator current signature. In the fault decision module, the fault diagnostic index from the FSDO estimator is used depending on the load conditions of the induction motors. Experimental results obtained in a 75 kW three-phase squirrel-cage induction motor show that the proposed diagnosis algorithm is capable of detecting BRB faults with an accuracy that is superior to a zoom multiple signal classification (ZMUSIC) and a zoom estimation of signal parameters via rotational invariance techniques (ZESPRIT).

Keywords: Broken rotor bar, Induction motor, Fault diagnosis, Current signal

1. Introduction

Induction motors are widely used in electrical machines in the electrical and processing industries. There are various induction motor failures from stator, rotor, bearing, or other faults [1, 2]. Induction motor failure results in severe damage to the motor itself, as well as to the motor-related processes in the industrial plant.

Many studies based on the frequency domain analysis using the fast Fourier transform (FFT) have been performed in order to detect broken rotor bars (BRBs), stator windings, and mechanical faults [3-6]. Using a motor current signature analysis (MCSA), which is based on the FFT method, the spectrum of stator currents can be used to diagnose BRBs faults and stator winding faults with various faulty motor conditions [3]. The MCSA based on the FFT analysis of the sideband components provides the information to diagnose accurately and quantitatively the broken rotor bars in induction machines [4]. A FFT-based MCSA with advanced signal-and-data-processing algorithms is proposed for an online induction motor diagnosis system [5]. A detection method is proposed for stator winding faults in the low-frequency-range of the flux spectrum with low resolution that exploits an external stray flux sensor [6]. However, the frequency resolution of FFT-based methods is limited to the number of data points.

Based on the FFT, zoom-FFT (ZFFT) techniques with window functions have been proposed to increase the frequency resolution [7-9]. ZFFT techniques reduce the computational time, save the memory size, and increase the accuracy in a specified frequency range [7-9]. However, the ZFFT techniques for the high-frequency resolution requires a long acquisition time [8, 9].

In the literature, time-frequency domain analyses based on wavelet-transform techniques have been investigated to overcome the resolution problem encountered in fault diagnostic analysis [10-12]. Wavelet-transform techniques, which are effective for stationary as well as nonstationary signal processing, provide a multiresolution signal analysis with high resolution in the time and frequency domains [10-12]. An automatic online diagnosis algorithm for broken-rotor-bar detection has been proposed based on the wavelet-transform application to the start-up current transient [10]. By using the wavelet decomposition, fault diagnosis has been performed in both time and frequency domains [11]. Based on a continuous wavelet technique with frequency B-spline functions, a diagnosis method identifies as many BRB fault-related frequency components as possible during large transients [12]. Wavelet-transform techniques can be applied to detect faults during stationary and non-stationary conditions [10-12]. However, in stationary conditions, wavelet-transform techniques have the disadvantage in the frequency resolution compared to the subspace methods.

Subspace methods such as a multiple signal classification (MUSIC) algorithm and an estimation of signal parameters via rotational invariance techniques (ESPRIT) have been applied to diagnose induction motor faults while overcoming the frequency resolution limitation of the FFT method in low signal-to-noise ratios (SNRs) [13-17]. The MUSIC and ESPRIT compute an auto-correlation matrix of the signals, estimate a frequency signal dimension order (FSDO), use signal and noise subspaces, and convert the fault detection problem into a generalized eigenvalue problem [13-17]. The MUSIC was

† Corresponding Author: Dept. of Electronic Engineering, Myongji University, Korea (yongkim@mju.ac.kr)
* HVDC Research Division, Korea Electrotechnology Research Institute (KERI), Korea ({dhhwang, ywyoun, jhsun}@keri.re.kr)
Received: April 9, 2013; Accepted: August 26, 2013

applied to estimate the harmonic components in order to improve induction motor fault detection [13]. The MUSIC and short-time MUSIC were used for the analysis of the space-vector of voltages induced in stator windings, after supply disconnection, to detect BRBs faults in induction machines [14]. The MUSIC algorithm with zooming methods was proposed to detect fault sensitive frequencies based on a frequency analysis of the stator current [15]. Using the motor leakage flux spectral analysis, the MUSIC is applied to identify BRB faults in induction motors [16]. The ESPRIT with the zooming technique has been proposed to estimate both the frequencies and amplitudes of BRB fault harmonics using the stator current analysis [17]. However, the difference in the spectrum of healthy motors and those with BRB faults determined using the zoom MUSIC (ZMUSIC) [15] or zoom ESPRIT (ZESPRIT) [17] is not obvious when the load level is close to no-load condition. To overcome this limitation, this paper proposes another fault diagnostic index using the result of the FSDO estimator, which is needed to perform the ZMUSIC [15] or ZESPRIT [17].

In experiments, the small slip induces small current flowing in the rotor even though under no-load condition [22, 23]. To detect BRBs faults under no-load condition, the wavelet transform is proposed using transient current analysis to overcome the resolution problem of FFT-based methods [22]. A detection method based on particle swarm optimization can estimate BRBs fault-related frequencies using stator current under no-load condition [23]. However, performance analysis using detection and false alarm probabilities is required in order to provide a stable diagnosis for BRBs faults [22, 23].

In this paper, a robust fault diagnosis algorithm is proposed to detect BRB faults in induction motors. In this approach, a FSDO estimator, and a fault decision module are proposed. For the FSDO estimator, we use the minimum description length (MDL) criterion [18] to improve the performance of BRB fault detection for motors operating with no load or a finite load. On the basis of the FSDO estimator, we propose a fault decision module that uses the FSDO estimate as a fault diagnosis index. In this module, the predetermined threshold values depending on the load conditions are optimized using the detection and false alarm probabilities from the experimental results. Experimental results show that the proposed diagnosis algorithm achieves the optimal performance for BRBs faults in various load conditions.

2. Detection of Broken Rotor Bar

In this section, frequencies in the current spectrum are analyzed in order to diagnose BRB faults. Then, a data model for BRB faults is presented using the stator current.

2.1 Frequency analysis of broken rotor bar

When an induction motor rotor bar is broken, the stator steady-state current has harmonic frequencies given by [15, 17]

$$f_{BRB} = (1 \pm 2ks) f_s, \tag{1}$$

where s is the per-unit motor slip, f_s is the electrical supply frequency, and k=1,2,3,… is the harmonic frequency index. In (1), the frequency of interest for BRB fault detection, f_{BRB}, exists near the electrical supply frequency f_s. Therefore, BRB faults are verified with the presence of frequency components of interest, f_{BRB}, near the electrical supply frequency, f_s, in the current spectrum.

The characteristic frequency for BRB fault detection, f_{BRB}, is a function of the slip s, where the slip s depends on the load condition [15, 17]. When the relative mechanical speed of the motor is almost the same as the motor synchronous speed, which occurs when the motor operates with no load, the slip s is very small and it is very hard to identify frequencies arising from BRB faults in (1) using the FFT method or the MUSIC algorithm [15, 17].

2.2 Data model

Discrete time-domain measurement data for the stator current can be represented as follows:

$$x[n] = s[n] + e[n] = \sum_{i=1}^{K} a_i \cos(2\pi f_i n + \phi_i) + e[n], \tag{2}$$

where $s[n]$ consists of sinusoids, $e[n]$ represents white noise with a zero mean and a variance of σ^2, K is the number of pure sinusoids, and a_i, f_i, and ϕ_i are the amplitude, the frequency, and the phase of the i th pure sinusoid, respectively. Using $\cos(2\pi f_i n + \phi_i) = \frac{1}{2}\left(e^{j(2\pi f_i n + \phi_i)} + e^{-j(2\pi f_i n + \phi_i)}\right)$ from Euler's formula [19], (2) can also be expressed in complex exponential form as

$$x[n] = s[n] + e[n] = \sum_{i=1}^{M} \bar{A}_i e^{j2\pi \bar{f}_i n} + e[n], \tag{3}$$

where $s[n] = \sum_{i=1}^{M} \bar{A}_i e^{j2\pi \bar{f}_i n}$, $\bar{A}_i = (\frac{a_i}{2}) e^{j\phi_i}$ for $1 \le i \le K$, $\bar{A}_{K+i} = (\frac{a_i}{2}) e^{-j\phi_i}$ for $1 \le i \le K$, $\bar{f}_i = f_i$ for $1 \le i \le K$, $\bar{f}_{K+i} = -f_i$ for $1 \le i \le K$, and $M = 2K$. Using $L > M$ serial discrete-time samples $\{x[n], x[n+1], \cdots, x[n+L-1]\}$, we can rewrite (3) in a compact matrix format as follows:

$$\mathbf{x}(n) = \mathbf{F}\bar{\mathbf{A}} + \mathbf{e}(n), \tag{4}$$

where $\mathbf{x}(n) = \left[x[n]\ x[n+1] \cdots x[n+L-1] \right]^T$,
$\mathbf{F} = [\mathbf{f}(\bar{f}_1)\ \mathbf{f}(\bar{f}_2) \cdots \mathbf{f}(\bar{f}_M)]$ with
$\mathbf{f}(\bar{f}_i) = [e^{j2\pi\bar{f}_i n}\ e^{j2\pi\bar{f}_i (n+1)} \cdots e^{j2\pi\bar{f}_i (n+L-1)}]^T$,
$i = 1,\ 2,\ \cdots,\ M$, $\bar{\mathbf{A}} = [\bar{A}_1\ \bar{A}_2 \cdots \bar{A}_M]^T$, and
$\mathbf{e}(n) = \left[e[n]\ e[n+1] \cdots e[n+L-1] \right]^T$.
Here, $\mathbf{F}$ is a $L \times M$ Vandermonde matrix of rank M and $\mathbf{f}(\bar{f}_i)$ is the mode vector with frequency $\bar{f}_i$, where $i = 1,\ 2, \cdots, M$.

3. BRB Fault Diagnosis Algorithm

In this section, a robust diagnosis scheme is proposed to detect BRB faults. The proposed diagnosis algorithm consists of a FSDO estimator, and a fault decision module. The FSDO estimator provides the number of frequency components in the measured data using the MDL criterion. A fault decision module uses the number of frequency components as the fault index to detect BRB faults.

3.1 FSDO estimator

The autocorrelation matrix $\mathbf{R}_x$ of the measurement data $\mathbf{x}(n)$ can be expressed as

$$\mathbf{R}_x = E\left[\mathbf{x}(n)\mathbf{x}^H(n) \right] = \mathbf{F}\mathbf{R}_{\bar{A}}\mathbf{F}^H + \sigma^2\mathbf{I}_L, \tag{5}$$

where $E[\cdot]$ denotes the expected value, $\mathbf{R}_{\bar{A}} = E\left[\bar{\mathbf{A}}\bar{\mathbf{A}}^H \right]$ denotes the signal correlation matrix, and $\mathbf{I}_L$ denotes an $L \times L$ identity matrix.

To implement the FSDO estimator, we need an estimate, $\hat{\mathbf{R}}_x$, of $\mathbf{R}_x$ in (5). By using $N > L$ serial measured time samples $\{x[n], x[n+1], \cdots, x[n+N-1]\}$, a spatial smoothing (SS) method is applied to calculate $\hat{\mathbf{R}}_x$ as follows [20]:

$$\hat{\mathbf{R}}_x = \frac{1}{P_s}\sum_{n=1}^{P_s} \mathbf{x}(n)\mathbf{x}^T(n), \tag{6}$$

where $P_s = N - L + 1$. In (6), the eigenvalues of $\hat{\mathbf{R}}_x$ is defined as $\{\lambda_1 \geq \lambda_2 \geq \cdots \geq \lambda_L\}$ and can be obtained using the eigenvalue decomposition. When $\hat{\mathbf{R}}_x$ has the full rank of M, we obtain

$$\lambda_1 \geq \lambda_2 \geq \cdots \geq \lambda_M > \lambda_{M+1} = \lambda_{M+2} = \cdots = \lambda_L = \sigma^2. \tag{7}$$

Information theoretic criteria, such as the MDL or Akaike information criterion (AIC), have been used to obtain the number of frequencies [18]. The MDL criterion for the estimation of M is used in this paper, and is given as follows [17, 18]:

$$MDL(k) = -\log\left(\frac{\prod_{i=k}^{L-1} \lambda_i^{\frac{1}{L-k}}}{\frac{1}{L-k}\sum_{i=k}^{L-1}\lambda_i} \right)^{P_s(L-k)} + \frac{1}{2}k(2L-k)\log(P_s). \tag{8}$$

The estimate of M can then be expressed as

$$\hat{M} = \arg_k \min MDL(k), \tag{9}$$

where $k = 0,1,\cdots,L-1$.

This estimate of M can be used to make a decision for the BRB fault detection. For example, when the no-load condition is satisfied, the slip s is 0.00022 and therefore the frequency estimation for harmonic frequencies in (1) cannot be performed precisely. However, when a faulty induction motor with a BRB fault operates in low load conditions, harmonic frequencies are introduced into the stator current due to the air-gap flux. Therefore, even though the difference between f_{BRB} and f_s is smaller than the frequency resolution of the frequency estimation, harmonic frequencies are present in the stator current in (1) for BRB faulty motors. In the proposed method, $\hat{M}$ is defined as a fault diagnostic index to detect BRB faults. The procedure for BRB fault detection is described in the following subsection.

3.2 Fault decision module

A functional block diagram of the proposed diagnosis scheme for BRB faults in induction motors is shown in Fig. 1. First, the measured data vector $\mathbf{x}(n)$ in (4) is used to calculate the autocorrelation matrix $\hat{\mathbf{R}}_x$ in (6). The eigenvalues of the correlation matrix are then computed. Through the analysis of the eigenvalues by the MDL criterion, the FSDO estimator calculates and supplies the estimate of the number of frequencies $\hat{M}$ in (9) to the fault decision module.

In the fault decision module, we use the property that $\hat{M}$ for BRB faulty motors is larger than that in healthy motors, because the BRB fault introduces harmonic frequencies in (1) in different load conditions. The fault decision module uses the motor speed R_S and $\hat{M}$ from the FSDO estimator. During the initial stage, the motor speed R_S can be estimated using the rotor-slot harmonics [5]. Let M_{th} be the threshold parameter predetermined from experimental results depending on the motor speed. At different load conditions, $\hat{M}$ in (9) is used for the BRB fault decision and is compared to M_{th}. This is because $\hat{M}$ increases even when the frequency estimation cannot be

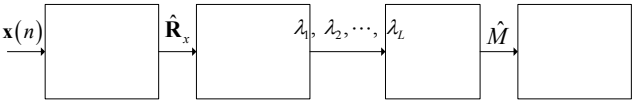

Fig. 1. Block diagram of the BRB fault diagnosis algorithm

performed exactly due to the low load condition [15, 17]. The proposed diagnosis algorithm detects BRB faulty motors with the optimal performance even at no load condition using M_{th}.

4. Experimental Results

In this section, we present our experimental setup and analyze the proposed BRB fault diagnosis algorithm with different motors and load conditions. For the fault decision module of the proposed method, the cumulative distribution functions (CDFs) for detection and false alarm probabilities obtained from experimental results. The performance of the proposed BRB fault diagnosis algorithm is compared with those of the ZMUSIC and ZESPRIT algorithms for different motors and under different load conditions.

4.1 Experimental setup

The experiment tests were performed with 75-kW squirrel-cage induction motors. Fig. 2 shows the induction motor test system, which is composed of a test motor, a load motor, an inverter, and a data acquisition system (DAS). The specifications of the test and load motors are described in Table 1. The inverter is connected to the load motor to control the load condition of the test motor. Three load conditions were considered: no-load, 50%, and 80% of the full load. Under the no-load, 50% load, and 80% load conditions, the slips are almost 0.00022, 0.0054, and 0.0091, respectively, and the speeds of the motor are 1799.6 rpm, 1791.3 rpm, and 1783.2 rpm, respectively. For

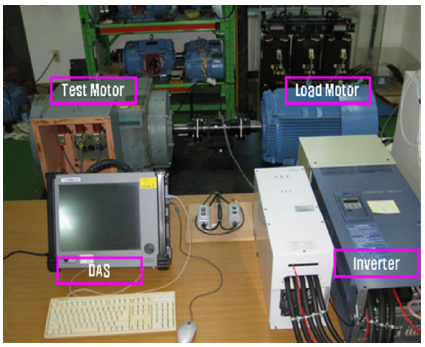

Fig. 2. Experimental setup

Table 1. Characteristics of the induction motor used in experiments

	Test motor	Load motor
Power	75 kW	75 kW
Voltage	3300 V	380 V
Current	16.8 A	139.4 A
Supply frequency	60 Hz	60 Hz
Number of poles	4	4
Speed	1778 rpm	1780 rpm

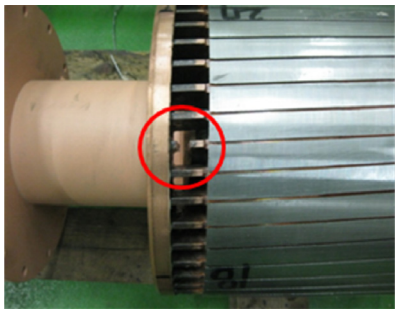

(a)

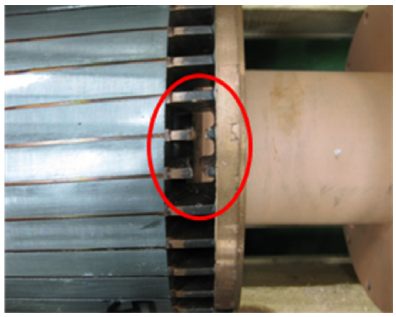

(b)

Fig. 3. BRB faults: (a) one BRB and (b) two BRBs

motor conditions, three types of motors were used: a healthy motor, a motor with one BRB, and a motor with two BRBs. As shown in Fig. 3, BRBs faults were simulated by cutting the end of the rotor bar.

The experimental data was gathered with a sampling rate f_d of 2 kHz. This can be achieved by downsampling 200 kHz sampled data from the DAS by an integer factor 100. This is because the BRB fault can be detected by the analysis of the frequency band near the electrical supply frequency f_s [15, 17]. For the FSDO estimator, the size of the correlation matrix, $L = 2048$, and the size of the measured time samples for the SS method, $N = 4096$, are used. The measurement data acquisition time is 2.048 seconds and the measurement data size is $N = 4096$. In order to verify the proposed diagnosis algorithm, the results are analyzed for all possible experimental cases.

4.2 Proposed BRB diagnosis algorithm

In the fault decision module, the fault diagnostic index $\hat{M}$ is exploited in order to detect BRB faults. Fig. 4 shows CDFs of the FSDO estimate $\hat{M}$ for healthy and faulty motors at the different load conditions. For the no-load condition, as shown in Fig. 4(a), there is a significant difference between the CDF of a healthy motor and the CDFs of faulty ones. Using the threshold value with $M_{th} = 163$ obtained from the CDF-based experimental results shown in Fig. 4(a), we can easily detect BRB faults in motors operating under the no-load with the false alarm probability for $\hat{M}$, i.e., $P_{FA,\hat{M}} = 0$, and the detection probability for $\hat{M}$, i.e., $P_{D,\hat{M}} = 1$, which are defined as

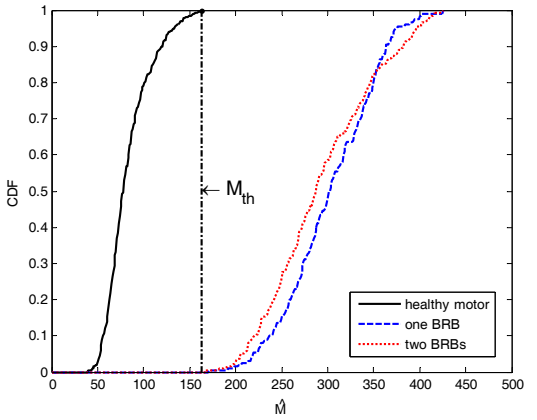

(a)

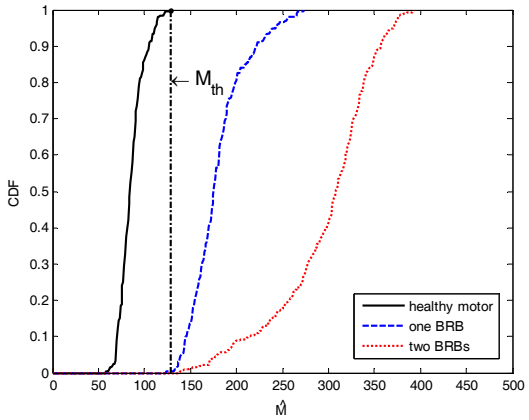

(b)

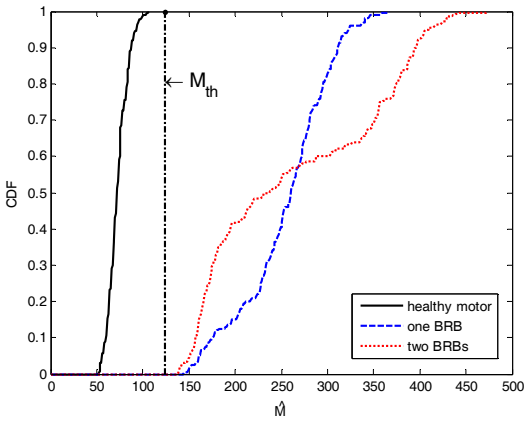

(c)

Fig. 4. CDFs of $\hat{M}$ for the (a) no-load, (b) 50% load, and (c) 80% load conditions. Threshold values are $M_{th}=163$, $M_{th}=128$, and $M_{th}=124$ for no-load, 50% load, and 80% load conditions, respectively.

follows [21]:

$$P_{FA,\hat{M}} = Pr\left\{\hat{M} > M_{th}; H_0\right\} \tag{10}$$

and

$$P_{D,\hat{M}} = Pr\left\{\hat{M} > M_{th}; H_1\right\} \tag{11}$$

where H_0 is the healthy motor hypothesis, and H_1 is the BRB faulty motor hypothesis. As shown in Figs. 4(b) and 4(c), the threshold values are determined to be $M_{th}=128$ for 50% load condition and to be $M_{th}=124$ for 80% load condition, respectively, using experimental results based on the CDFs of healthy and faulty motors. Using the threshold values, BRB faults under 50% and 80% load conditions can be easily detected using $\hat{M}$ with $P_{FA,\hat{M}}=0$ and $P_{D,\hat{M}}=1$. Therefore, for the fault decision module, the fault index $\hat{M}$ can be used for the no-load and finite load conditions.

Fig. 5 shows the threshold values as a function of load rates, D, using experimental results. As predicted by the experimental results as shown in Fig. 4, the threshold value M_{th} decreases as the load rate D increases. This is because when the load rate D increases, the motor slip s increases and the BRBs fault-related frequencies f_{BRB} in (1) are getting away from the electrical supply frequency, therefore the number of BRBs fault-related frequencies from the autocorrelation matrix of measured data in (5) decreases. Moreover, lines with two different slopes can be calculated with a small set of samples. The absolute value of slope between no-load and 50 % load conditions is larger than that between 50 % and 80 % load conditions.

For comparison purposes, the ZMUSIC [15] and ZESPRIT [17] have been analyzed at no-load condition. For the ZMUSIC, the frequency shift was -60 Hz, the acquisition time was 3 s, and the 100 Hz sampling frequency data, which can be obtained by downsampling 200 kHz sampled data from the DAS by an integer factor 2000. For the ZESPRIT, the acquisition time was 3 s, and the 200 Hz sampling frequency data, which can be obtained by downsampling 200 kHz sampled data from the DAS by an integer factor 1000. The fault index A_M^L is defined as the amplitude of lower side band harmonic (LSH) in bandwidth $BW1$ of the pseudospectrum for the ZMUSIC, where the fault index is computed with respect to the noise level [15]. The fault index A_B^S for the

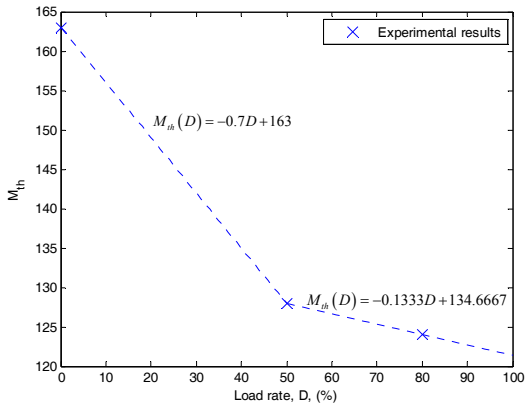

Fig. 5. Threshold values as a function of load rate D.

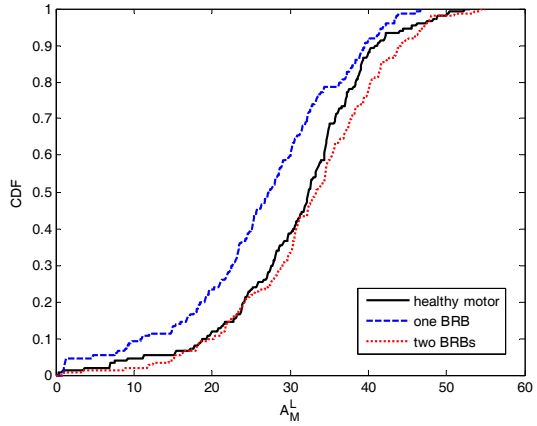

(a)

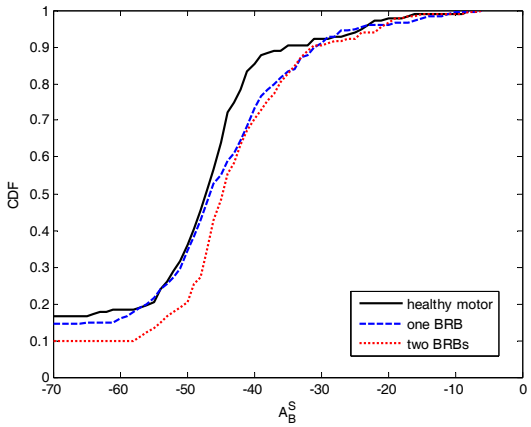

(b)

Fig. 6. CDFs at no-load condition. (a) Fault index A_M^L in $\mathrm{BW1} = [57,\ 60\ \mathrm{Hz}]$ for the ZMUSIC [15], (b) Fault index A_B^S in $BW1 = [57,\ 60\ \mathrm{Hz}]$ and $BW2 = [60,\ 63\ \mathrm{Hz}]$ for the ZEPSRIT [17].

ZEPSRIT is defined as the sum of amplitudes of LSH in bandwidth $BW1$ and upper sideband harmonic (USH) in bandwidth $BW2$ [17].

Fig. 6 shows the CDFs of fault indices A_M^L and A_B^S for ZMUSIC [15] and ZESPRIT [17], respectively, for no-load condition where the slip s is 0.00022 and the motor speed is 1799.6 rpm. For fault indices, the bandwidth $BW1$ is between 57 and 60 Hz, and the bandwidth $BW2$ is between 60 and 63 Hz. For the ZMUSIC as shown in Fig. 6(a), the CDF of A_M^L for the healthy motor is between those for the faulty motor with one BRB and two BRBs.

For the ZESPRIT as shown in Fig. 6(b), the CDF of A_B^S for the healthy motor is close to those for faulty motors with one BRB and two BRBs. Compared to Fig. 4(a), the ZMUSIC and ZESPRIT cannot detect the BRB fault frequencies at the no-load condition due to the fault-related frequency f_{BRB} is almost the same with the electrical supply frequency f_s.

Furthermore, under the 50% and 80% load conditions as shown in Figs. 4(b) and 4(c), the proposed BRB fault diagnosis algorithm has better performance for the detection probability $P_{D,\hat{M}}$ and false alarm probability $P_{FA,\hat{M}}$ compared to those of ZMUSIC and ZESPRIT [17]. Therefore, compared to the ZMUSIC and ZESPRIT [17], the proposed BRB fault diagnosis algorithm accurately detects BRB faulty motors under no load and finite load conditions.

5. Conclusion

In this paper, an accurate and efficient diagnosis algorithm is proposed for BRB fault detection in three-phase squirrel-cage induction motors under no-load and finite load conditions. Fault diagnostic index from the FSDO estimator is proposed considering the stator current signature based on all fault sensitive frequencies. Experimental results show that the proposed diagnosis algorithm provides the optimal performance under no-load and finite load conditions of induction motor.

The main advantages of the proposed diagnosis algorithm are that it can correctly identify BRB faults using a few samples and can be easily implemented using software. The main drawback, which is also found in other high-resolution spectral analysis methods such as the MUSIC, ZMUSIC and ZESPRIT, is that the FSDO estimator is limited to the steady-state operating condition of the induction motor.

Acknowledgements

This work was supported in part by the "Development of Motor Diagnosis Technology for the Electric Vehicle" project of Korea Electrotechnology Research Institute (KERI) and in part by the Human Resources Development program (No. 20114010203030) of the Korea Institute of Energy Technology Evaluation and Planning(KETEP) grant funded by the Korea government Ministry of Trade, Industry and Energy.

References

[1] M. R. W. Group, "Report of large motor reliability survey of industrial and commercial installation, Part II," *IEEE Trans. Ind. Appl.*, vol. IA-21, no. 4, pp. 865-872, July/Aug. 1985.

[2] M. E. H. Benbouzid, "A review of induction motors signature analysis as a medium for faults detection," *IEEE Trans. Ind. Electron.*, vol. 47, no. 5, pp. 984-993, Oct. 2000.

[3] W. T. Thomson and M. Fenger, "Current signature analysis to detect induction motor faults," *IEEE Ind. Appl. Mag.*, vol. 7, no. 4, pp. 26-34, July/Aug. 2001.

[4] A. Bellini, F. Filippetti, G. Franceschini, C. Tassoni, and G. B. Kliman, "Quantitative evaluation of

induction motor broken bars by means of electrical signature analysis," *IEEE Trans. Ind. Appl.*, vol. 37, no. 5, pp.1248-1255, Sept./Oct. 2001.

[5] J.-H. Jung, J.-J Lee, and B.-H. Kwon, "Online diagnosis of induction motors using MCSA," *IEEE Trans. Ind. Electron.*, vol. 53, no. 6, pp. 1842-1852, Dec. 2006.

[6] H. Henao, C. Demian, and G.-A. Capolino, "A frequency-domain detection of stator winding faults in induction machines using an external flux sensor," *IEEE Trans. Ind. Appl.*, vol. 39, no. 5, pp. 1272-1279, Sept./Oct. 2003.

[7] J. L. Zarader, M. Garnier, and M. Nicollet, "New frequency-filtering zoom," *Int. J. Adapt. Control Signal Process.*, vol. 6, no. 6, pp. 547-560, Jun. 1992.

[8] A. Yazidi, H. Henao, G. A. Capolino, M. Artioli, and F. Filippetti, "Improvement of frequency resolution for three-phase induction machine fault diagnosis," in Proc. 40th IAS Annu. Meeting. Conf. Rec., 2005, vol. 1, pp. 20-25.

[9] A. Bellini, A. Yazidi, F. Filippetti, C. Rossi, and G.-A. Capolino, "High frequency resolution techniques for rotor fault detection of induction machines," *IEEE Trans. Ind. Electron.*, vol. 55, no. 12, pp. 4200-4209, Dec. 2008.

[10] A. Ordaz-Moreno, R. de Jesus Romero-Troncoso, J. A. Vite-Frias, J. R. Rivera-Gillen, and A. Garcia-Perez, "Automatic online diagnosis algorithm for broken-bar detection on induction motors based on discrete wavelet transform for FPGA implementation," *IEEE Trans. Ind. Electron.*, vol. 55, no. 5, pp. 2193-2202, May 2008.

[11] A. Bouzida, O. Touhami, R. Ibtiouen, A. Belouchrani, M. Fadel, and A. Rezzoug, "Fault diagnosis in industrial induction machines through discrete wavelet transform," *IEEE Trans. Ind. Electron.*, vol. 58, no. 9, pp. 4385-4395, Sept. 2011.

[12] J. Pons-Llinares, J. A. Antonino-Daviu, M. Riera-Guasp, M. Pineda-Sanchez, and V. Climente-Alarcon, "Induction motor diagnosis based on a transient current analytic wavelet transform via frequency B-splines," *IEEE Trans. Ind. Electron.*, vol. 58, no. 5, pp. 1530-1544, May 2011.

[13] M. E. H. Benbouzid, M. Vieira, and C. Theys, "Induction motors' faults detection and localization using stator current advanced signal processing techniques," *IEEE Trans. Power Electron.*, vol. 14, no. 1, pp. 14-22, Jan. 1999.

[14] F. Cupertino, E. de Vanna, L. Salvatore, and S. Stasi, "Analysis techniques for detection of IM broken rotor bars after supply disconnection," *IEEE Trans. Ind. Appl.*, vol. 40, no. 2, pp. 526-533, Mar./Apr. 2004.

[15] S. H. Kia, H. Henao, and G.-A. Capolino, "A high-resolution frequency estimation method for three-phase induction machine fault detection," *IEEE Trans. Ind. Electron.*, vol. 54, no. 4, pp. 2305-2314, Aug. 2007.

[16] Y.-Y. Youn, S.-H. Yi, D.-H. Hwang, J.-H. Sun, D.-S. Kang, and Y.-H. Kim, "MUSIC-based diagnosis algorithm for identifying broken rotor bar faults in induction motors using flux signal," *Journal of Electrical Engineering and Technology*, vol. 8, no. 2, pp. 288-294, Mar. 2013.

[17] Y.-H. Kim, Y.-W. Youn, D.-H. Hwang, J.-H. Sun, and D.-S. Kang, "High-resolution parameter estimation method to identify broken rotor bar faults in induction motors," *IEEE Trans. Ind. Electron.*, will be published.

[18] M. Wax and T. Kailath, "Detection of signals by information theoretic criteria," *IEEE Trans. Acoust., Speech and Signal Process.*, vol. ASSP-33, no. 2, pp. 387-392, Apr. 1985.

[19] G. Strang, Calculus. Wellesley-Cambridge, 1991.

[20] M. Kristensson, M. Jansson, and B. Ottersten, "Further results and insights on subspace based sinusoidal frequency estimation," *IEEE Trans. Signal Process.*, vol. 49, no. 12, pp. 2962-2974, Dec. 2001.

[21] S. M. Kay, Fundamentals of statistical signal processing: detection theory. Englewood Cliffs, NJ: Prentice-Hall, 1993.

[22] K. M. Siddiqui, and V. K. Giri, "Broken rotor bar fault detection in induction motors using wavelet transform," in Proc. Computing, Electronics and Electrical Technologies (ICCEET), 2012, pp. 1-6.

[23] V. Rashtchi, and R. Aghmasheh, "A new method for identifying broken rotor bars in squirrel cage induction motor based on particle swarm optimization method," *World academy of science, engineering and technology*, vol. 43, pp. 694-698, July 2010.

Don-Ha Hwang received B.S., M.S., and Ph.D. degrees in Electrical Engineering from Yeungnam University in 1991, 1993, and 2003, respectively. He is currently a principal researcher at Korea Electrotechnology Research Institute (KERI), Changwon, Korea. His main research interest are design, analysis, monitoring, and diagnosis of electric machines.

Young-Woo Youn received B.S. and M.S. degrees in Communication Engineering from Information and Communication University, Daejeon, Korea, in 2005 and 2007, respectively. He is currently a researcher at power apparatus research center at Korea Electrotechnology Research Institute (KERI), Changwon, Korea. His research interests are in condition monitoring and signal processing.

Jong-Ho Sun received B.S., M.S., and Ph.D. degrees in Electrical Engineering from Pusan National University in 1986, 1988, and 2001, respectively. Currently, he is a principal researcher at Korea Electrotechnology Research Institute (KERI), Changwon, Korea. His interests are diagnosis techniques for electric power equipments.

Yong-Hwa Kim received a B.S. in electrical engineering in 2001 from Seoul National University, Seoul, Korea, and a Ph. D. in electrical and computer engineering from Seoul National University, Seoul, Korea, 2007. From 2007 to 2011, he was a senior researcher with the Korea Electro-technology Research Institute (KERI), Geonggi-do, Korea. From 2011 to 2013, he was an assistant professor at the Division of Maritime Electronic and Communication Engineering, Mokpo National Maritime University, Korea. Since March 2013, he has joined the faculty with the Department of Electronic Engineering at Myongji University, Korea. His general research interests include communi-cation systems, motor drives and diagnosis, and digital signal processing. Currently, he is particularly interested in communications and digital signal processing for Smart Grid.